

# Experimental demonstration of a 10 Gb/s RSOA-based 16-QAM subcarrier multiplexed WDM PON

Jonathan M. Buset,<sup>1,\*</sup> Ziad A. El-Sahn,<sup>1,2</sup> and David V. Plant<sup>1</sup>

<sup>1</sup>Photonics Systems Group, Department of Electrical and Computer Engineering,  
McGill University, Montréal, QC H3A 2A7, Canada

<sup>2</sup>Electrical Engineering Department, Alexandria University, Alexandria 21544, Egypt

\*[jonathan.buset@mail.mcgill.ca](mailto:jonathan.buset@mail.mcgill.ca)

**Abstract:** We experimentally demonstrate the performance of a 10 Gb/s subcarrier multiplexed (SCM) wavelength-division multiplexed (WDM) passive optical network (PON) using 2.5 Gbaud 16-QAM transmission signals. Digital signal processing (DSP) and square-root raised cosine (SRRC) pulse shaping enable both the uplink and downlink channels to achieve net spectral efficiencies up to 2.8 bit/s/Hz per channel using reflective semiconductor optical amplifier (RSOA)-based optical network units (ONUs) and economical 10 GHz intensity modulation and direct detection transceivers. We characterize the system's bit error rate (BER) performance over a 20 km single feeder PON with both remote continuous-wave (CW) seeding and full-duplex transmission scenarios, assuming standard forward error correction (FEC) codes.

© 2013 Optical Society of America

**OCIS codes:** (060.0060) Fiber optics and optical communications; (060.2330) Fiber optics communications; (060.2360) Fiber optics links and subsystems; (060.4510) Optical communications.

---

## References and links

1. "Cisco Visual Networking Index: Forecast and Methodology, 2012–2017," Tech. Rep., Cisco Inc. (2013).
2. D. Breuer, C. Lange, E. Weis, M. Eiselt, M. Roppelt, K. Grobe, J.-P. Elbers, S. Dahlfors, F. Cavaliere, and D. Hood, "Requirements and solutions for next-generation access," in *Proceedings of ITG Symposium on Photonic Networks* (IEEE, 2011), pp. 1–8, paper 12.
3. K. Y. Cho, Y. Takushima, and Y. C. Chung, "10-Gb/s operation of RSOA for WDM PON," *IEEE Photon. Technol. Lett.* **20**, 1533–1535 (2008).
4. J. Prat, "Rayleigh back-scattering reduction by means of quantized feedback equalization in WDM-PONs," in *Proceedings of European Conference on Optical Communication* (IEEE, 2010), pp. 1–3, paper Th.10.B.3.
5. I. Papagiannakis, M. Omella, D. Klonidis, A. Birbas, J. Kikidis, I. Tomkos, and J. Prat, "Investigation of 10-Gb/s RSOA-based upstream transmission in WDM-PONs utilizing optical filtering and electronic equalization," *IEEE Photon. Technol. Lett.* **20**, 2168–2170 (2008).
6. H. Kim, "10-Gb/s operation of RSOA using a delay interferometer," *IEEE Photon. Technol. Lett.* **22**, 1379–1381 (2010).
7. M. Presi, A. Chiuchiarelli, R. Corsini, P. Choudury, F. Bottoni, L. Giorgi, and E. Ciaramella, "Enhanced 10 Gb/s operations of directly modulated reflective semiconductor optical amplifiers without electronic equalization," *Opt. Express* **20**, B507–B512 (2012).
8. K. Roberts, D. Beckett, D. Boertjes, J. Berthold, and C. Laperle, "100G and beyond with digital coherent signal processing," *IEEE Commun. Mag.* **48**, 62–69 (2010).
9. N. Yoshimoto, J. Kani, S.-Y. Kim, N. Iiyama, and J. Terada, "DSP-based optical access approaches for enhancing NG-PON2 systems," *IEEE Commun. Mag.* **51**, 58–64 (2013).
10. N. Cvijetic, "OFDM for next-generation optical access networks," *J. Lightw. Technol.* **30**, 384–398 (2012).

11. K. Y. Cho, U. H. Hong, S. P. Jung, Y. Takushima, A. Agata, T. Sano, Y. Horiuchi, M. Suzuki, and Y. C. Chung, "Long-reach 10-Gb/s RSOA-based WDM PON employing QPSK signal and coherent receiver," *Opt. Express* **20**, 15353–15358 (2012).
12. D. Lavery, M. Ionescu, S. Makovejs, E. Torrenco, and S. J. Savory, "A long-reach ultra-dense 10 Gbit/s WDM-PON using a digital coherent receiver," *Opt. Express* **18**, 25855–25860 (2010).
13. J. M. Buset, Z. A. El-Sahn, and D. V. Plant, "Experimental demonstration of a 10 Gb/s subcarrier multiplexed WDM PON," *IEEE Photon. Technol. Lett.* **25**, 1435–1438 (2013).
14. C. Arellano, K. Langer, and J. Prat, "Reflections and multiple Rayleigh backscattering in WDM single-fiber loopback access networks," *J. Lightwave Technol.* **27**, 12–18 (2009).
15. K. Y. Cho, A. Murakami, Y. Lee, A. Agata, Y. Takushima, and Y. C. Chung, "Demonstration of RSOA-based WDM PON operating at symmetric rate of 1.25 Gb/s with high reflection tolerance," in *Proceedings of Optical Fiber Communication Conference (OSA/IEEE, 2008)*, paper OTuH4.
16. Z. Al-Qazwini and H. Kim, "Symmetric 10-Gb/s WDM-PON using directly modulated lasers for downlink and RSOAs for uplink," *J. Lightwave Technol.* **30**, 1891–1899 (2012).
17. J. M. Buset, Z. A. El-Sahn, and D. V. Plant, "Demonstration of a symmetric 10 Gb/s QPSK subcarrier multiplexed WDM PON with IM/DD transceivers and a bandwidth-limited RSOA," in *Proceedings of National Fiber Optic Engineers Conference (OSA/IEEE, 2013)*, paper NTh4F.1.
18. T. Duong, N. Genay, P. Chanclou, B. Charbonnier, A. Pizzinat, and R. Brenot, "Experimental demonstration of 10 Gbit/s upstream transmission by remote modulation of 1 GHz RSOA using adaptively modulated optical OFDM for WDM-PON single fiber architecture," in *Proceedings of European Conference on Optical Communication (IEEE, 2008)*, pp. 1–2, paper Th.3.F.1.
19. M.-K. Hong, N. C. Tran, Y. Shi, J.-M. Joo, E. Tangdiongga, S.-K. Han, and A. M. J. Koonen, "10-Gb/s transmission over 20-km single fiber link using 1-GHz RSOA by discrete multitone with multiple access," *Opt. Express* **19**, B486–B495 (2011).
20. J. M. Buset, Z. A. El-Sahn, and D. V. Plant, "Experimental demonstration of a 10 Gb/s 16-QAM SCM WDM PON with bandwidth-limited RSOA and IM/DD transceivers," in *Proceedings of European Conference on Optical Communication (IEEE, 2013)*, pp. 1–3, paper Tu.3.F.5.
21. Y. Wang, E. Serpedin, and P. Ciblat, "An alternative blind feedforward symbol timing estimator using two samples per symbol," *IEEE Trans. Commun.* **51**, 1451–1455 (2003).
22. J. L. Wei, E. Hugues-Salas, R. P. Giddings, X. Q. Jin, X. Zheng, S. Mansoor, and J. M. Tang, "Wavelength reused bidirectional transmission of adaptively modulated optical OFDM signals in WDM-PONs incorporating SOA and RSOA intensity modulators," *Opt. Express* **18**, 9791–9808 (2010).
23. J. G. Proakis and M. Salehi, *Digital Communications*, 5th ed. (McGraw Hill, 2007).
24. A. Chiuchiarelli, M. Presi, R. Proietti, G. Contestabile, P. Choudhury, L. Giorgi, and E. Ciaramella, "Enhancing resilience to Rayleigh crosstalk by means of line coding and electrical filtering," *IEEE Photon. Technol. Lett.* **22**, 85–87 (2010).

---

## 1. Introduction

The data capacity of access networks must continue to evolve to meet consumer appetites for high bandwidth services such as streaming Internet video, video-on-demand and cloud-based storage [1]. These popular, data intensive services will drive the adoption of fiber-to-the-home by network providers to meet the need for greater capacity on access networks.

Future passive optical networks (PONs) using time-division multiplexing (TDM) will provide a short term upgrade pathway for operators to increase the total shared bandwidth available to users, but scaling TDM-based networks beyond 10 Gb/s is expected to be technically challenging [2]. Wavelength-division multiplexed (WDM) PONs are expected to provide the necessary bandwidth capacities in the long term, and should require only minimal upgrades to the existing infrastructure in order to provide an economically viable upgrade path from current TDM PONs. A single feeder architecture should be maintained, while the passive power splitter at the remote node (RN) will be replaced by an athermal arrayed waveguide grating (AWG). Client-side colourless optical network units (ONUs) will be essential to reduce inventory complexity for the network operator. The reflective semiconductor optical amplifier (RSOA) is a well studied candidate for colourless ONU transmitters and although their modulation bandwidth is fundamentally limited to less than 3 GHz, RSOAs can be operated at 10 Gb/s or greater data rates using a variety of electrical [3, 4] and optical [5–7] equalization techniques.

In transport level networks, digital signal processing (DSP) is proven to be an effective means

of replacing expensive optical components with high-speed transceiver electronics [8]. There is great potential to achieve significant performance gains in access networks from economical optoelectronic transceivers using DSP in next generation PON solutions [9–13].

In bidirectional PONs with downlink remodulation, the uplink channel performance is primarily limited by Rayleigh backscattering (RB), reflections and inter-channel crosstalk [14]. Radio frequency (RF) subcarrier multiplexing (SCM) is a simple and effective means of reducing their impact [15]. Previously, SCM solutions required high bandwidth receivers [16] to achieve symmetric 10 Gb/s data rates. Recently the authors demonstrated SCM WDM PON architectures using higher order modulation and pulse shaping to achieve symmetric 10 Gb/s channels within 10 GHz of electrical bandwidth [13, 17]. In both cases, the uplink channel was limited to 5 Gbaud QPSK.

Other PON techniques also pair DSP and higher order modulation formats to improve the spectral efficiency and overcome the RSOA bandwidth limitation. Orthogonal frequency division multiplexing (OFDM) [10, 18] and discrete multi-tone (DMT) [19] are two approaches that use many subcarriers at lower baud rates to carry the channel data. These multi-carrier approaches provide flexibility in terms of per user bandwidth allocation, but can require more complex DSP at the transmitter and receiver to process the parallel data streams. In our SCM WDM PON approach each channel is placed on a single subcarrier enabling serial signal processing using standard DSP techniques.

In this investigation we extend the concepts of our initial demonstration [20] and present the performance of a symmetric 10 Gb/s per wavelength 16-QAM SCM WDM PON using a bandwidth-limited RSOA-based ONU and economical intensity modulation (IM)/direct detection (DD) optoelectronics. In contrast to previous demonstrations, here we use 16-QAM signals on both the uplink and downlink to increase the net spectral efficiency up to 2.8 bit/s/Hz per channel. This enables guard bands to separate the SCM channels from surrounding noise sources. The RSOA's 2.2 GHz modulation bandwidth is spectrally pre-compensated in DSP, while offset optical filtering is used at the optical line terminal (OLT) to further enhance the chirped upstream signal [13, 17]. The implementation of a new receiver DSP block to correct for timing and sampling frequency offset (SFO) improves both the uplink BER floor and receiver sensitivity, while reducing the timing sensitivities due to signal pulse shaping. We demonstrate operation over a single feeder 20 km WDM PON and characterize the system in terms of bit error ratio (BER) performance. We also present scenarios with both remote continuous-wave (CW) seeding and wavelength reuse of the modulated downlink signal. We then demonstrate symmetric operation at 5 dBm of OLT launch power and achieve a  $-12.5$  dBm minimum receiver power sensitivity for the uplink, assuming standard Reed-Solomon (RS) forward error correction (FEC) codes with 12.5% overhead.

## 2. PON physical architecture

Figure 1 illustrates the single feeder architecture we used in this investigation. The OLT transmitter consists of a Micram VEGA digital-to-analog converter (DAC) with 6 bit precision driving an electro-absorption modulated laser (EML) centred at 1549.41 nm. Following the EML, a booster erbium-doped fiber amplifier (EDFA) and variable optical attenuator (VOA) control the launch power  $P_{OLT\_Tx}$ , as measured at the circulator's port 2 output. The downlink extinction ratio is set with a bias-tee to achieve a minimum BER. The optical distribution network (ODN) comprises a 20.35 km feeder of standard single mode fiber (SMF-28e+), a 100 GHz AWG and a 1.5 km distribution drop fiber (DDF). The ODN losses are 9.19 dB.

At the ONU, 70% of the downstream signal is tapped off for detection by the receiver comprised of a p-i-n photoreceiver, a RF amplifier and a real-time oscilloscope (Agilent DSOX96204Q) performing 8 bit precision analog-to-digital conversion (ADC). The remain-

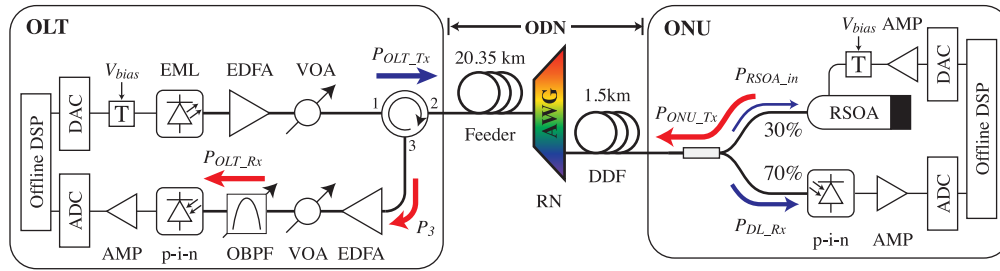


Fig. 1. Physical architecture of the SCM WDM PON. The optimized 70/30 ONU coupler balances the power budgets. AMP: RF amplifier, EML: electro-absorption modulated laser (CyOptics E4560), OBPF: 0.3 nm optical band-pass filter (JDSU VCF050), p-i-n: 10 GHz photoreceiver (DSC-R402), RN: remote node, RSOA: reflective semiconductor optical amplifier (CIP SOA-RL-OEC-1550), T: RF bias-tee.

ing 30% of the downstream signal seeds a RSOA with peak gain from 1530 nm to 1570 nm and 2.2 GHz modulation bandwidth. The RSOA uplink transmitter is directly modulated at  $4 V_{p-p}$ , biased at 80 mA, and is driven by a second VEGA DAC. At the OLT, an EDFA pre-amplifies the upstream signal prior to detection and a VOA sets the input power to the p-i-n,  $P_{OLT\_Rx}$ . In a real-world deployment the EDFA cost would be shared among the PON's user base. Optical filter detuning has been shown to increase the RSOA's effective bandwidth by transforming the unwanted phase modulation due to the device's transient chirp into IM [5]. Here, an optical band pass filter (OBPF) is offset from the carrier wavelength by  $-0.18$  nm [13] to optically enhance the received signal while also emulating a second AWG for wavelength demultiplexing [7]. The OLT receiver is similar to that of the ONU consisting of a p-i-n photoreceiver, a RF amplifier and an ADC to capture the received signal.

### 3. DSP enabled 10 Gb/s 16-QAM channels

Figure 2 outlines the general flow of the transmitter and receiver software stacks [13, 17]. At the transmitters,  $2^{23} - 1$  and  $2^{31} - 1$  length pseudo-random bit sequences are generated offline for the downlink and uplink, respectively, and a short preamble is added to the start of each sequence. After 16-QAM symbol mapping the sequences are truncated to 512 kSymbol to match the DAC memory depth. A square-root raised cosine (SRRC) filter then increases the signal's spectral efficiency and reduces the effects of intersymbol interference (ISI). The null-to-null electrical bandwidth of the pulse shaped channel is  $B_{ch} = (1 + \alpha_{ch}) \times R_{sym}$ , where  $\alpha_{ch}$  is the SRRC roll off factor and  $R_{sym}$  is the symbol rate. To facilitate the transmission of high order 16-QAM electrical signals with low-cost optoelectronics, a finite impulse response (FIR) filter pre-compensates for each channel's bandwidth limiting component by flattening the power spectrum over the band of interest [13]. The DACs then drive the optical transmitters with the 6 bit quantized signals.

The data stream captured at 40 GSa/s by the ADC receiver is downsampled, RF down-converted and a matched SRRC filter removes ISI and out-of-band noise. A block based on 2 Sa/Symbol blind feedforward symbol timing estimation [21] then corrects for timing and sampling frequency offset (SFO). After the QAM decision blocks, the preamble symbols are used to remove phase ambiguity of the phase-locked loop (PLL) output. At the OLT receiver, post-compensation is optionally performed using a decision feedback equalizer (DFE) with 12 forward and 1 backward symbol-spaced taps. The DFE taps are initially trained using the preamble symbols and then dynamically adjusted using the least-mean square (LMS) algorithm. The signal is then demodulated for BER calculation using  $\sim 3.5 \times 10^6$  bit of data.

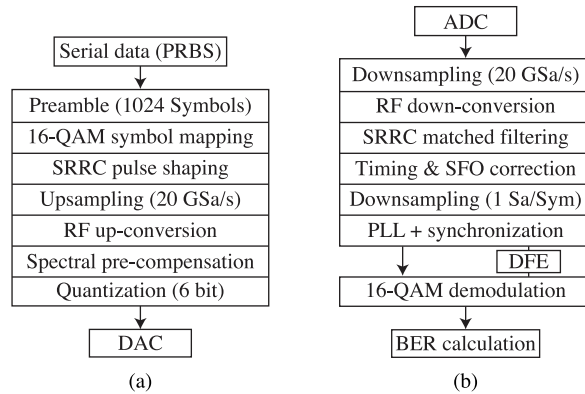


Fig. 2. Block diagrams of the (a) transmitter and (b) receiver DSP stacks used for offline processing of the downlink and uplink signals. Note that DFE post-compensation is optionally performed at the OLT receiver, but is not used at the ONU to reduce complexity.

## 4. Experimental results and discussion

### 4.1. Downlink

The downlink channel is a 2.5 Gbaud 16-QAM signal on a 7.97 GHz RF subcarrier. A 16th order FIR filter pre-compensates for the bandwidth roll off of both the EML transmitter and 10 GHz ONU p-i-n photoreceiver. In Fig. 3 we confirm the downlink channel operation by characterizing its BER performance as a function of  $P_{OLT\_Tx}$ . A BER threshold of  $1.1 \times 10^{-3}$  is assumed for RS(255,223) FEC. Additionally, different SRRC roll off factors  $\alpha_{DL}$  are tested to vary the channel's bandwidth and spectral efficiency.

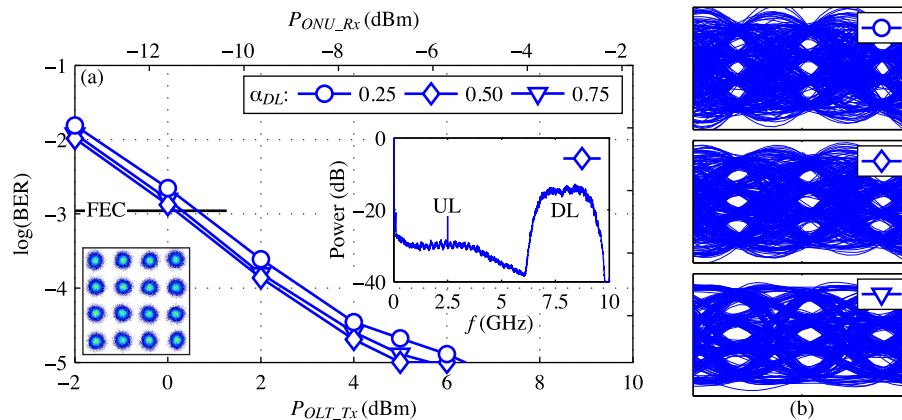


Fig. 3. (a) Downlink channel BER after transmission over a 20 km PON. The received power is also presented for completeness (top x-axis). A normalized electrical power spectrum and example constellation at  $P_{OLT\_Tx} = 5$  dBm are inset. We note the presence of uplink channel noise from simultaneous upstream transmission. (b) Eye diagrams of the in phase 16-QAM signal component for different  $\alpha_{DL}$ .

As the OLT launch power increases, the downlink BER quickly reaches below the FEC threshold for powers greater than 1 dBm, corresponding to a receiver sensitivity of  $-11$  dBm. Increasing the launch power beyond 5 dBm results in BERs below the  $\sim 10^{-5}$  calculation floor.

This behaviour corresponds with previous demonstrations [13]. All of the roll off factors tested performed similarly in terms of BER and sensitivity. The highest spectral efficiency tested is 3.2 bit/s/Hz when  $\alpha_{DL} = 0.25$ , resulting in a channel bandwidth of 3.125 GHz. After accounting for the RS(255,223) overhead, the information spectral efficiency is reduced to 2.8 bit/s/Hz.

The eye diagrams in Fig. 3(b) demonstrate the effect of  $\alpha_{DL}$  on the signal in the time domain. A larger roll off factor broadens the pulse width in time and in turn increases the eye opening of the multilevel signal. A smaller  $\alpha_{DL}$  value decreases the pulse width and the channel's bandwidth, but leads to increased timing sensitivity at the receiver. In this case, the impact of  $\alpha_{DL}$  is minimized by adding a timing and SFO correction block in the DSP stack.

#### 4.2. Uplink

The uplink channel is a 2.5 Gbaud 16-QAM signal on a 2.97 GHz RF subcarrier. A 64th order FIR filter pre-compensates for the RSOA bandwidth roll off prior to quantization. The OLT launch power  $P_{OLT\_Tx}$  was fixed at 5 dBm while characterizing the performance of the upstream transmission. As shown above in Fig. 3, this launch power provides an excellent downlink performance while staying below the threshold power for stimulated Brillouin scattering (SBS) [22]. This  $P_{OLT\_Tx}$  corresponds to a RSOA input power  $P_{RSOA\_in} = -10.7$  dBm, which is greater than the RSOA's saturation power of  $-17$  dBm. The ONU gain is  $\sim 12.9$  dB resulting in an upstream  $P_{ONU\_Tx} = 2.2$  dBm. After transmission through the ODN, the received power at port 3 of the circulator is measured to be  $P_3 = -7.6$  dBm.

In Fig. 4 we present the BER performance of the 10 Gb/s upstream transmission with both remote CW seeding and symmetric transmission with wavelength reuse from a portion of the modulated downlink signal. The impact of the uplink SRRC roll off factor is verified for  $\alpha_{UL}$  from 0.25 to 1.00, with resulting channel bandwidths ranging from 3.125 GHz to 5 GHz, respectively. The downlink  $\alpha_{DL}$  was fixed at 0.50 for symmetric operation.

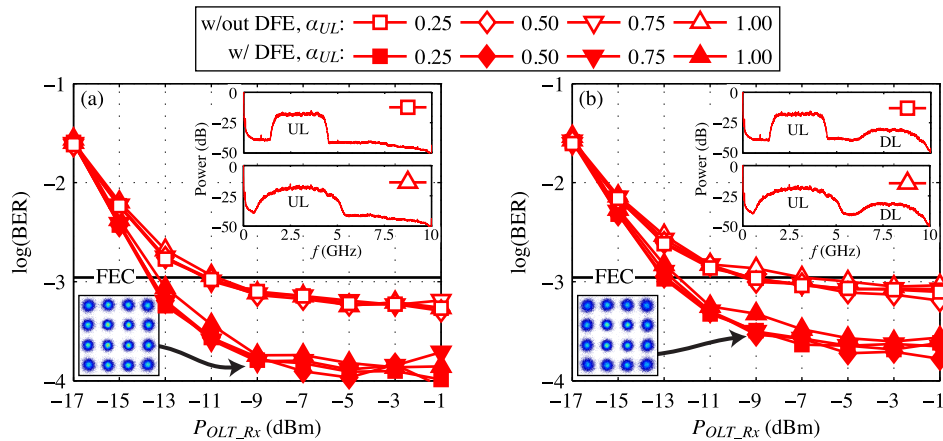


Fig. 4. Uplink BER performance of the upstream after transmission over a 20 km PON with (a) CW seeding, and (b) full-duplex transmission. Normalized electrical power spectra are inset, as well as an equalized constellation for  $\alpha_{UL} = 0.25$ .

In Fig. 4(a), the uplink with remote CW seeding achieves a BER below the FEC threshold at  $-11$  dBm of received power. This represents a 2 dB improvement over our initial demonstration [20] due to the new timing and SFO correction block. The addition of a DFE eliminates any residual ISI and further reduces the sensitivity to  $-13.5$  dBm. In both cases the BER performance reaches a floor for received powers greater than  $-9$  dBm due to noise limitations.

Figure 4(b) demonstrates the uplink performance during full-duplex transmission. As a result of reusing the modulated downlink signal, the penalty is only a  $\sim 1.5\times$  increase in BER. On the other hand, the uplink receiver sensitivity degrades to  $-7$  dBm without post-compensation, a 4 dB power penalty compared to the CW seeding case. Adding a post-compensation DFE block at the OLT receiver removes any residual ISI in the uplink signal and significantly improves the receiver sensitivity, requiring just  $-12.5$  dBm of power to operate below the FEC threshold. In terms of power penalty, the difference between CW seeding and symmetric transmission is reduced to only 1 dB when a DFE is used at the OLT receiver. Similar to the downlink channel, the uplink performance is quite insensitive to roll off for  $\alpha_{UL} \geq 0.25$ . For the remaining analysis, we will assume the use of a DFE at the OLT receiver in order to maintain BERs well below the FEC threshold.

### 4.3. Comparison with the Shannon limit

Figure 5(a) is an example of the BER performance of both the downlink and uplink channels with respect to  $E_b/N_0$ , the signal to noise ratio (SNR) per bit of information after the FEC overhead has been removed [23]. To calculate  $E_b/N_0$  for each data set, the frequency domain spectrum is first calculated from the captured time domain signals. Integrating over the channel bandwidth and subtracting the average noise power from the signal results in the gross SNR per symbol,  $E_s/N_0$ . The SNR per bit of information is then given by

$$\frac{E_b}{N_0} = \frac{E_s}{N_0} \frac{1}{\log_2(M)} \frac{n}{k}, \quad (1)$$

where  $M = 16$  is the QAM order and  $(n, k) = (255, 223)$  are the block lengths for the RS FEC coding.

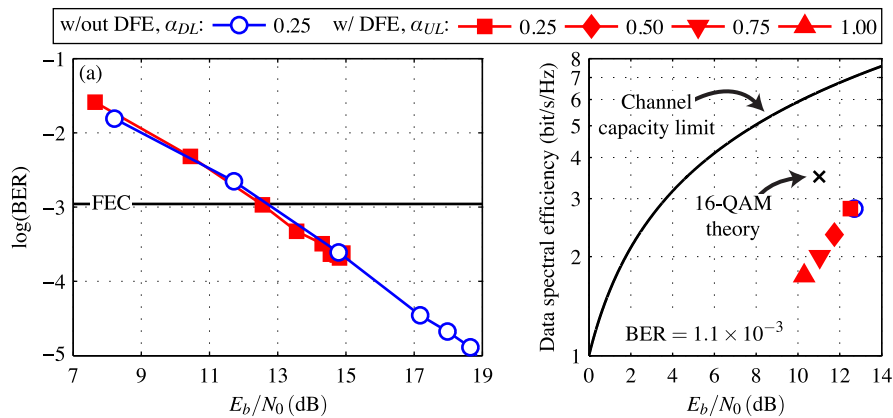


Fig. 5. (a) BER vs.  $E_b/N_0$  for the downlink and uplink channels. (b) Comparison of the 16-QAM SCM WDM PON performance with different SRRC roll off factors to Shannon's channel capacity limit. We also include the best theoretical 16-QAM RS(255,223) FEC coded signal to achieve the BER threshold [23]. Note that the added overhead for the RS(255,223) FEC has been taken into account for both the spectral efficiency and  $E_b/N_0$ .

For the downlink channel, we see that as  $E_b/N_0$  increases with launch power and the BER steadily drops below the FEC threshold at 12.7 dB. The uplink BER reaches below the FEC threshold at  $E_b/N_0 = 12.5$  dB. In this case,  $E_b/N_0$  does not increase beyond 15 dB because the uplink signal power is limited by the gain saturated RSOA.

Furthermore, in Fig. 5(b) we can use these  $E_b/N_0$  values to compare the performance of this SCM WDM PON with Shannon's channel capacity limit [23],  $E_b/N_0 > \frac{2^r-1}{r}$ , where  $r$  is the channel's spectral efficiency. Here the design trade off between bandwidth and energy is evident, as the highest spectral efficiency requires  $\sim 2.2$  dB greater  $E_b/N_0$  than the lowest one.

#### 4.4. Discussion

This 16-QAM SCM WDM PON solution improves on previous demonstrations [13, 17] by increasing the channels' net spectral efficiency up to 2.8 bit/s/Hz, while still maintaining a simple wavelength reuse scheme and commodity IM/DD transceivers at both the OLT and ONU. Guard bands of up to 1 GHz ( $\alpha_{UL} = 0.25$ ) isolate the uplink channel from surrounding noise sources, including low frequency RB beat noise [24] and inter-channel crosstalk from the downlink signal [14]. The noise can then be efficiently filtered out in DSP during the down-conversion and SRRC matched filtering stages. Notably, these improvements are achieved without any additional optical components or significant impact to the channel's BER compared to previous demonstrations.

Although 2.8 bit/s/Hz is the highest net spectral efficiency achieved in this investigation, it is not necessarily the highest possible. As evident in Fig. 5(b), increasing the uplink channel's spectral efficiency further would require larger  $E_b/N_0$ . This, however, could prove difficult given that the maximum value obtained in this investigation was  $\sim 15$  dB. Achieving a larger  $E_b/N_0$  by increasing  $P_{OLT\_Tx}$  beyond 5 dBm would limit any gains because of additional RB and SBS [13]. Further reducing  $\alpha$  also narrows the eye opening and increases the receiver's sensitivity to timing jitter. At 10 Gb/s data rates,  $\alpha = 0.25$  provides adequate guard bands to separate the data channels from noise and crosstalk without impacting performance. The architecture's flexibility allows the signal bandwidths to be engineered to achieve the network operator's quality of service (QoS) requirements. In the future, this could open the possibility of increasing baud rates, or possibly mixing and matching the QAM order, baud rate and pulse shaping to achieve the network operator's desired specifications.

## 5. Conclusion

In this paper we present a 10 Gb/s SCM WDM PON architecture using DSP to maximize the performance of economical IM/DD transceivers, achieving net spectral efficiencies up to 2.8 bit/s/Hz per channel. We characterize the system's performance over a single feeder 20 km PON with both remote CW seeding and full-duplex transmission scenarios and achieve BERs below the RS(255,223) FEC threshold. The pulse shaped 16-QAM channels facilitate guard bands, providing robust resistance to upstream impairments and leading to a small 1 dB power penalty for reusing the downlink modulated signal as a seed source. To the best of our knowledge this is the highest reported spectral efficiency for a 10 Gb/s SCM WDM PON.